

## NOTATION

$P_0$	is the injection pressure in injector capillary;
$P_r$	is the pressure at exit from receptor capillary;
$P_{0\max}$	is the pressure in injector capillary with jet at the stability threshold;
$P_{r\max}$	is the pressure in receptor capillary with jet at the stability threshold;
$l$	is the distance between orifices of injector and receptor capillaries;
$L$	is the distance from capillary axis to reflecting surface;
$d$	is the inside diameter of capillary;
$\omega$	is the acoustic frequency;
$Re = ud/\nu$	is the Reynolds number;
$u$	is the average flow velocity;
$\nu$	is the kinematic viscosity;
$St = u/\omega l$	is the Strouhal number.

## LITERATURE CITED

1. V. N. Dmitriev and V. G. Gradetskii, Fundamentals of Pneumatic Automation [in Russian], Mashinostroenie, Moscow (1971).
2. V. N. Zhigulev, A. I. Kirkinskii, V. N. Sidorenko, and A. M. Tumilin, "Mechanism of secondary instability and its role in the process of inception of turbulence," in: Aeromechanics [in Russian], Nauka, Moscow (1976).
3. M. T. Landahl, "Wave mechanics of breakdown," J. Fluid Mech., 52, No. 4 (1972).

## FRICTION AND THE VELOCITY AND GAS-CONTENT PROFILES OF A TURBULENT GAS - LIQUID FLOW

A. V. Gorin

UDC 532.529.5

The limiting relative friction law is used to derive analytical expressions for the frictional stress as well as the velocity and gas-content distributions in the cross section of a boundary layer and a pipe.

Only a limited number of theoretical papers to date has any attempt been made to solve the problem of calculating the hydrodynamic characteristics associated with the turbulent flow of gas-liquid mixtures. In the majority of those papers the two-phase system is regarded as a locally homogeneous medium amenable to the methods and assumptions commonly used in the theory of single-phase turbulent flows. For example, Bankoff [1] postulates that the tangential stress is uniform throughout the channel cross section and the mixing length is the same as for single-phase turbulent flow. Brown and Kranich [2] use a logarithmic distribution function for the velocity of the mixture in the bubble-flow regime, neglecting the relative velocity between the phases. Beattie [3] treats the bubbles as cavities distributed in proportion to the velocity distribution of the liquid and adopts the same assumptions as in [1]. Levy [4] has derived distributions of the velocity and density of the mixture and the pressure drop on the basis of Van Driest's modification of mixing-length theory. Here the turbulent constants are considered to be the same as for single-phase liquid flow. Sato and Sekoguchi [5] regard the bubbles as cavities, the presence of which has the effect of creating fluctuations of the liquid velocity (over and above the independently existing single-phase turbulent fluctuations of the liquid velocity) due to flow around bubbles. This process induces additional turbulent stresses. The bubble function is considered to be a given quantity. Kashcheev and Muranov [6] have calculated the velocity profile of a mixture for annular-mist flow, replacing the two-phase core by a homogeneous flow and invoking the basic assumptions of semi-empirical turbulence theories.

The fundamental problem that arises in the realization of a locally homogeneous model is whether or not it is justified to use the turbulence constants for single-phase flow. Tong [7], for example, concludes on the

---

Translated from *Inzhenerno-Fizicheskii Zhurnal*, Vol. 35, No. 3, pp. 415-423, September, 1978. Original article submitted June 27, 1977.

basis of an analysis of the experimental data that the value of the mixing-length constant at a certain distance from the wall is much smaller than for the single-phase liquid.

In the present article we calculate the friction losses and of velocity and gas-content distributions of the mixture in the cross section of the flow channel on the basis of the theory of the limiting relative friction law developed for a turbulent boundary layer of a compressible gas.

We regard an isothermal two-phase system as a continuum with physical properties that depend on the gas content, and for the turbulent frictional stress  $\tau$  we use the equation [4]

$$\tau = \bar{\rho} \overline{u'v'} + \bar{u} \bar{\rho}' \overline{v'}, \quad (1)$$

in which the overbar signifies time averaging in the customary sense for turbulence problems.

The fluctuation components are determined as follows in accordance with mixing-length theory (on the assumption that the turbulent transfer of momentum and density is identical):

$$u' = v' = l (d\bar{u}/dy), \quad \rho' = l (d\bar{\rho}/dy);$$

the transverse coordinate  $y$  is measured away from the plate (channel wall).

Substituting these expressions into Eq. (1), we obtain

$$\tau = l^2 \frac{d\bar{u}}{dy} \frac{d\bar{\rho}\bar{u}}{dy}. \quad (2)$$

To determine the relationship between  $\bar{\rho}$  and  $\bar{u}$  (we drop the overbar from now on) we assume similarity of the velocity and mass-concentration fields:

$$\frac{u}{u_m} = \frac{c - c_w}{c_m - c_w}. \quad (3)$$

The following expression holds for the local density of the two-phase system:

$$\rho = \rho_l (1 - \varphi) + \rho_g \varphi.$$

The volume concentration  $\varphi$  is related to the mass concentration  $c$  by the equation

$$c = \varphi \rho_g / \rho. \quad (4)$$

From expressions (3) and (4) we obtain for the density of the medium (assuming that  $c_w = 0$ )

$$\rho = \frac{\rho_l}{1 - A(u/u_m)}. \quad (5)$$

Here  $A = 1 - \rho_l/\rho_m$ .

Thus, on the basis of (5) we can write Eq. (2) in the form

$$\tau = \rho_l \left( \frac{l}{1 - Au/u_m} \frac{du}{dy} \right)^2. \quad (6)$$

We use the relative formulation of [8, 9] for the friction law, generalized in [10]. As the "standard" flow we take an incompressible fluid flow with parameters corresponding to the values for our compressible fluid at the outer boundary of the boundary layer (channel axis). Hereinafter we designate the standard-flow parameters by subscript zero.

We introduce the dimensionless variables

$$\omega = u/u_m; \quad \tilde{\tau} = \tau/\tau_w; \quad \tilde{l} = l/\delta; \quad \tilde{\xi} = y/\delta; \quad c_f = 2\tau_w/\rho_m u_m^2,$$

whereupon Eq. (6) acquires the form

$$\left( \frac{c_{f0}}{2} \tilde{\tau}_0 \right)^{1/2} \frac{d\tilde{\xi}}{\tilde{l}_0} = \left( \frac{\rho_l}{\rho_m} \frac{\tilde{\tau}_0}{\tilde{\tau}} \frac{1}{\Psi} \right)^{1/2} \frac{\tilde{l}}{\tilde{l}_0} \frac{d\omega}{1 - A\omega}, \quad (7)$$

with

$$\Psi = (c_f/c_{f0})_{\text{Re}}. \quad (8)$$

In (8) the comparison is made for  $Re = idem$ .

We integrate Eq. (7) across the layer so that

$$Z\Psi^{1/2} = \left(\frac{\rho_l}{\rho_m}\right)^{1/2} \int_{\omega_1}^1 \frac{\tilde{l}}{\tilde{l}_0} \left(\frac{\tilde{\tau}_0}{\tilde{\tau}}\right)^{1/2} \frac{d\omega}{1-A\omega}, \quad (9)$$

where

$$Z = (c_{f0}/2)^{1/2} \int_{\xi_1}^1 (\tilde{\tau}_0^{1/2}/\tilde{l}_0) d\xi.$$

It has been shown [8] that as  $Re \rightarrow \infty$  the quantities  $\omega_1 \rightarrow 0$ ,  $\xi_1 \rightarrow 0$ , and  $Z \rightarrow 1$ . We postulate that

$$\tilde{\tau}_0/\tilde{\tau} = 1, \quad \tilde{l}/\tilde{l}_0 = k = \text{const}, \quad (10)$$

and  $k$  characterizes the influence of the "second" phase on the mixing length in the mixture. It then follows from (9) that as  $Re \rightarrow \infty$

$$\Psi_\infty = \frac{\rho_l}{\rho_m} \left[ \frac{k \ln(\rho_m/\rho_l)}{1 - \rho_l/\rho_m} \right]^2. \quad (11)$$

We now obtain the velocity and density distributions of the medium. Integrating Eq. (7), we write

$$\left(\frac{\rho_l}{\rho_m}\right)^{1/2} \int_{\omega}^1 \frac{\tilde{l}}{\tilde{l}_0} \left(\frac{\tilde{\tau}_0}{\tilde{\tau}} \frac{1}{\Psi}\right)^{1/2} \frac{d\omega}{1-A\omega} = \int_{\xi}^1 \left(\frac{c_{f0}}{2} \tilde{\tau}_0\right)^{1/2} \frac{d\xi}{\tilde{l}_0}. \quad (12)$$

It has been shown [9] that

$$\int_{\xi}^1 \left(\frac{c_{f0}}{2} \tilde{\tau}_0\right)^{1/2} \frac{d\xi}{\tilde{l}_0} \Big|_{Re \rightarrow \infty} = 1 - \omega_0, \quad (13)$$

where  $\omega_0 = (1 + 1/\kappa_0)(c_{f0}/2)^{1/2} \ln \xi$  is the dimensionless velocity under standard conditions and  $\kappa_0$  is the Kármán constant for single-phase flow. Equation (12) therefore takes the form

$$\left(\frac{\rho_l}{\rho_m}\right)^{1/2} \int_{\omega}^1 \frac{\tilde{l}}{\tilde{l}_0} \left(\frac{\tilde{\tau}_0}{\tilde{\tau}} \frac{1}{\Psi}\right)^{1/2} \frac{d\omega}{1-A\omega} = 1 - \omega_0.$$

For large values of the Reynolds number Eq. (13) goes over to the limiting expression, so that as  $Re \rightarrow \infty$  we obtain approximately

$$\int_{\omega}^1 \frac{\tilde{l}}{\tilde{l}_0} \left(\frac{\tilde{\tau}_0}{\tilde{\tau}}\right)^{1/2} \frac{d\omega}{1-A\omega} = -\Psi_\infty^{1/2} \frac{1}{\kappa_0} \left(\frac{c_{f0}}{2}\right)^{1/2} \ln \xi,$$

whence, bearing relations (10) and (11) and mind, we readily deduce

$$\omega = \left(1 - \xi^n \frac{\rho_l}{\rho_m}\right) / \left(1 - \rho_l/\rho_m\right), \quad (14)$$

where the power exponent  $n$  is given by the expression

$$n = -\frac{1}{\kappa_0} \left(\frac{c_{f0}}{2}\right)^{1/2} \ln \left(\frac{\rho_m}{\rho_l}\right).$$

For the density distribution across the layer (channel) we have, according to (5),

$$\rho = \rho_m \xi^{-n}.$$

The distribution of the concentration obeys the law

$$\varphi = \left(1 - \frac{\rho_m}{\rho_l} \xi^{-n}\right) / \left(1 - \frac{\rho_g}{\rho_l}\right). \quad (15)$$

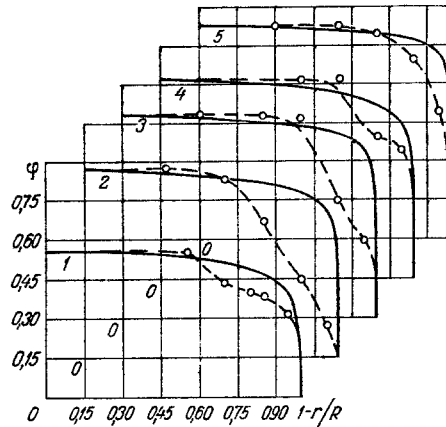


Fig. 1. Comparison of calculated true gas-content profiles (solid curves) with experimental data of [12] (points). 1)  $d = 24$  mm,  $w_0^I = 0.5$  m/sec,  $w_0^{II} = 1.44$  m/sec; 2) 24 mm, 1.5 m/sec, 2.83 m/sec; 3) 69 mm, 1.5 mm/sec, 3.4 m/sec; 4) 24 mm, 0.5 m/sec, 4.69 m/sec; 5) 69 mm, 1.5 m/sec, 5.94 m/sec.

We note that in plotting the velocity and gas-content profiles it is not necessary to know  $k$ , because it cancels out in the course of the computations.

The foregoing analysis is valid for a pipe or for a plane channel.

We now consider the case of a circular pipe of radius  $R$ . The values of  $\rho_m$  and  $u_m$  on the pipe axis are found in terms of the mass flow rate of the gas  $G_g$  and the total mass flow rate of the gas and liquid  $G$ . We define the average pipe-flow characteristics as follows:

1) the average density of the mixture  $\langle \rho \rangle$  is defined as

$$\langle \rho \rangle = 2 \int_0^1 (1 - \xi) \rho d\xi = \frac{2\rho_m}{(1-n)(2-n)},$$

where  $\xi = y/R$ ;

2) the cross-section average velocity of the mixture  $\langle u \rangle$  has the form

$$\langle u \rangle = \frac{u_m}{1 - \rho_l/\rho_m} \left[ 1 - \frac{\rho_l}{\rho_m} \frac{2}{(1+n)(2+n)} \right]; \quad (16)$$

3) the total mass flow rate  $G$  across unit area is

$$G = 2 \int_0^1 (1 - \xi) \rho u d\xi = \frac{\rho_l u_m}{1 - \rho_l/\rho_m} \left[ \frac{\langle \rho \rangle}{\rho_l} - 1 \right]; \quad (17)$$

4) the mass flow rate of the gas  $G_g$  across unit area can be determined from the relation

$$G_g = 2\rho_g \int_0^1 (1 - \xi) \varphi u d\xi,$$

so that the relative mass-flow gas content is given by the expression

$$X = \frac{G_g}{G} = \frac{u_m/\langle u \rangle}{\rho_l/\rho_g - 1} \cdot \frac{1 - \rho_l/\rho_m}{\langle \rho \rangle/\rho_l - 1}. \quad (18)$$

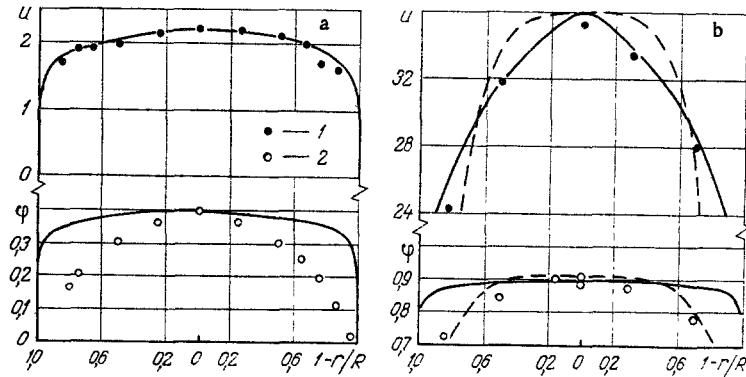


Fig. 2. Comparison of calculated velocity ( $u$ , m/sec) and gas-content profiles (solid curves) with experimental data of [3]. 1) Velocity; 2) gas concentration; a)  $d = 80$  mm,  $G = 1000$  kg/m<sup>2</sup>sec,  $\langle \varphi \rangle = 0.211$ ,  $P = 20.2 \cdot 10^5$  N/m<sup>2</sup>; b)  $d = 25.1$  mm,  $G = 3799$  kg/m<sup>2</sup>sec,  $X = 0.155$ ,  $P = 50 \cdot 10^5$  N/m<sup>2</sup>; dashed curves: approximation curves from [11],  $\varphi/\varphi_m = 1 - \xi^{5.88}$ ;  $u/u_m = 1 - \xi^{3.77}$ .

For stabilized pipe flow the expression for  $\Psi_\infty$  must be written with regard for the ratio  $\langle u_m \rangle / \langle u \rangle$ , because in boundary-layer theory the coefficient of friction is referred to the maximum velocity; for pipe flow this coefficient is referred to the mass-flow average velocity. On the basis of these considerations we write for stabilized conditions

$$\Psi_\infty = \left[ \frac{\tau_w}{\rho_m u_m^2} / \left( \frac{\tau_w}{\rho_m u_m^2} \right)_0 \right]_{\text{Re}} = \left[ \frac{\tau_w}{\rho_m \langle u \rangle^2} / \left( \frac{\tau_w}{\rho_m \langle u \rangle^2} \right)_0 \right]_{\text{Re}} \left[ \frac{\langle u \rangle}{u_m} / \left( \frac{\langle u \rangle}{u_m} \right)_0 \right]^2,$$

whence with regard for (16) we obtain

$$\bar{\Psi}_\infty = \left[ \frac{\xi}{\xi_0} \right]_{\text{Re}} = \Psi_\infty \left[ \frac{1 - \rho_l/\rho_m}{1 - 2\rho_l/\rho_m (1+n)^{-1} (2+n)^{-1}} \right]^2 h^2,$$

where  $h = (\langle u \rangle / u_m)_0$ ;  $\xi = 2\tau_w / (\rho_m \langle u \rangle^2)$ .

The graphical dependence of  $h$  on  $\text{Re}$  for isothermal flow in smooth pipes is given in [8]. The relation for the exponent in the velocity and gas-content distributions takes the form

$$n = - \frac{h}{2\alpha_0} \left( \frac{\xi_0}{2} \right)^{1/2} \ln \left( \frac{\rho_m}{\rho_l} \right). \quad (19)$$

Solving Eqs. (17) and (18) with regard for the expression (19) for  $n$ , we can determine  $\rho_m$  and  $u_m$ .

The profiles obtained for the velocity (14) and the true gas content (15) with the exponent  $n$  calculated according to (19) are compared in Figs. 1 and 2 with certain experimental data [3, 12]. The friction coefficient  $\xi_0$  is determined according to Prandtl law

$$\xi_0^{-1/2} = 2 \lg (\text{Re} \xi_0^{1/2}) - 0.8, \quad \text{Re} = 2GR/\mu_l.$$

As is evident from the graphs, the theory predicts a relatively flat distribution of the true volume concentration of gas  $\varphi$  in the pipe cross section (Fig. 1). Some discrepancies of the calculated profiles in the immediate wall zone are to be expected, because the calculations are carried out for  $\text{Re} \rightarrow \infty$ , making it possible to exclude the viscous sublayer from consideration, but error is nonetheless introduced. It is important to note the good agreement between theory and experiment for the velocity distribution of the gas-liquid mixture (Fig. 2).

Using the expressions derived above for the average flow characteristics of a gas-liquid mixture, we obtain an expression for the Martinelli dimensionless group  $\Phi_{L0}^2$ , defined as follows:

$$\frac{8\tau_w}{\rho_l (G/\rho_l)^2} = \Phi_{L0}^2 \lambda. \quad (20)$$

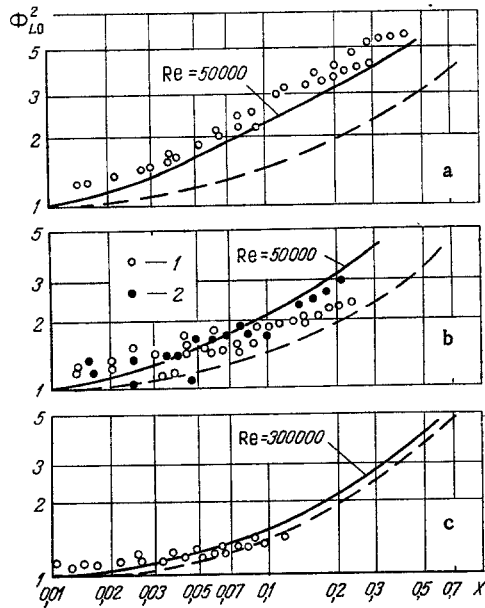


Fig. 3. Comparison of the results of friction calculations (dashed curves) with the calculations of Levy (solid curves) and experimental data [4] for flow of boiling water in a vertical channel at  $P = 140 \cdot 10^5 \text{ N/m}^2$ . a)  $G = 3.4 \cdot 10^6 \text{ kg/m}^2\text{h}$ ,  $Re = 53,000$ , channel dimensions  $690 \text{ mm} \times 25.4 \text{ mm} \times 2.5 \text{ mm}$ ; b)  $G = 7.3 \cdot 10^6 \text{ kg/m}^2\text{h}$ ; 1) channel  $690 \text{ mm} \times 25.4 \text{ mm} \times 2.5 \text{ mm}$ ;  $Re = 112,000$ ; 2) channel  $690 \text{ mm} \times 25.4 \text{ mm} \times 1.3 \text{ mm}$ ,  $Re = 60,000$ ; c)  $G = 19.5 \cdot 10^6 \text{ kg/m}^2\text{h}$ ,  $Re = 300,000$ , channel  $690 \text{ mm} \times 25.4 \text{ mm} \times 2.5 \text{ mm}$ .

where  $\lambda$  is the friction coefficient for single-phase fluid flow with total mass flow

$$\tau_{0G} = \frac{1}{8} \lambda \rho_l (G/\rho_l)^2,$$

which corresponds to the tangential stress for single-phase liquid flow, and

$$\Phi_{L0}^2 = \tau_w / \tau_{0G}. \quad (21)$$

Using relation (17) for the mass flow rate per unit area, we obtain

$$\frac{8\tau_w}{\rho_l (G/\rho_l)^2} = \frac{8\beta^2 \kappa_0^2}{(1 - \langle \rho \rangle / \rho_l)^2}. \quad (22)$$

Here  $\beta = \rho_l - \rho_m / \rho_m u_m 1 / \kappa_0 (\tau_w / \rho_l)^{1/2}$  is a parameter introduced by Levy. Let us examine it in closer detail. We represent it in the form

$$\beta = \left( \frac{\rho_l}{\rho_m} - 1 \right) \frac{1}{\kappa_0} \left( \frac{\tau_w}{\tau_0} \frac{\tau_0}{\rho_m u_m^2} \frac{\rho_m}{\rho_l} \right)^{1/2} = - \frac{A}{\kappa_0} \left( \frac{\rho_m}{\rho_l} \frac{c_{f0}}{2} \Psi \right)^{1/2}.$$

For large values of the Reynolds number  $\Psi \rightarrow \Psi_\infty$ , and for  $\beta$  we obtain approximately  $\beta = kn$ . We finally have

$$\Phi_{L0}^2 \lambda = 8k^2 n^2 \kappa_0^2 \left[ 1 - \frac{\rho_m}{\rho_l} \frac{2}{(1-n)(2-n)} \right]^{-2}. \quad (23)$$

The results of our calculation of the Martinelli parameter  $\Phi_{L0}^2$  (dashed curves) according to (23) for  $k = 1$  are compared in Fig. 3 with the calculations of Levy [4] (solid curves) and the experimental data of Sher and

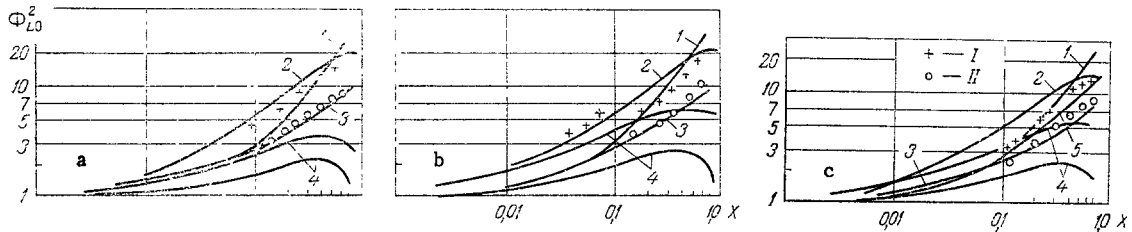


Fig. 4. Comparison of the results of friction calculations with experimental data of Muscettola from [7] (a, b) and [13] (c) and with the results of other authors for  $P = 70 \cdot 10^5 \text{ N/m}^2$ . a)  $d = 5 \text{ mm}$ : I)  $G = 11.5 \text{ kg/m}^2\text{sec}$ ,  $Re = 5000$ ; II)  $G = 43.7 \text{ kg/m}^2\text{sec}$ ,  $Re = 22,700$ ; b)  $d = 10.1 \text{ mm}$ : I)  $G = 11.0 \text{ kg/m}^2\text{sec}$ ,  $Re = 11,500$ ; II)  $G = 31.8 \text{ kg/m}^2\text{sec}$ ,  $Re = 33,400$ ; c)  $d = 8.2 \text{ mm}$ : I)  $G = 10.7 \text{ kg/m}^2\text{sec}$ ,  $Re = 9100$ ; II)  $G = 40.1 \text{ kg/m}^2\text{sec}$ ,  $Re = 34,200$ ; 1) data of Levy; 2) Martinelli and Nelson; 3) present calculation; 4) Marchaterre; 5) Thom.

Green [4]. It is evident from the figure that for sufficiently large Reynolds numbers good agreement is obtained between the experimental and calculated values.

Figure 4 gives the results of our calculations and selected experimental data of Muscettola cited in [7] (Fig. 4a, 4b) and [13] (Fig. 4c), along with semiempirical dependences and correlations of various authors, taken from the same literature sources. It is seen that the calculations describe the experimental data with varying degrees of accuracy. The discrepancy of the experimental results with Levy's relation can be attributed primarily to the fact that the latter ignores the dependence on the mass flow rate.

The results of calculations according to Marchaterre's relation, in which an attempt is made to account for the influence of  $G$  and  $d$ , exhibit poor agreement with the experimental data, mainly because of a strong dependence on the pipe diameter. This dependence is not so marked in the experimental results.

Calculations based on Martinelli and Nelson's relation, in which again the dependence on the mass flow rate is ignored, are in much better agreement with the experimental. The discrepancy increases, however, with the value of the mass flow rate.

The agreement between the results of our calculations and the experimental data, on the other hand, improves with increasing mass flow rate. The mass flow enters into the expression for  $\Phi_{L0}^2$  in terms of the drag coefficients, but scarcely any stratification with respect to  $G$  is observed.

#### NOTATION

$y$	is the transverse coordinate;
$u, v$	are the longitudinal and transverse velocity components;
$\rho$	is the density;
$\tau$	is the frictional stress;
$l$	is the mixing length;
$c, \varphi$	are the mass and volume concentrations, respectively;
$\delta$	is the boundary layer thickness;
$\Phi_{L0}^2$	is the Martinelli parameter;
$d$	is the pipe diameter;
$\kappa$	is the Kármán constant;
$G$	is the mass flow rate per unit area;
$c_f, \zeta$	are the coefficients of friction in boundary-layer and pipe flows;
$\mu$	is the dynamic viscosity;
$w_0', w_0''$	are the reduced velocities of liquid and gas;
$X$	is the relative mass-flow gas content;
$P$	is the pressure;
'	refers to fluctuation component.

#### Indices

$m, w$	are the parameters at upper boundary of boundary layer (or pipe axis) and wall;
$l, g$	are the liquid and gas;
0	is the standard flow.

## LITERATURE CITED

1. S. G. Bankoff, *Trans. ASME, Ser. C: J. Heat Transfer*, 82, No. 4 (1960).
2. F. G. Brown and W. Z. Kranich, *AIChE. J.*, 14, No. 5 (1968).
3. D. R. H. Beattie, *Nucl. Eng. Design*, 21, No. 1 (1972).
4. S. Levy, *Trans. ASME, Ser. C: J. Heat Transfer*, 85, No. 2 (1963).
5. Y. Sato and K. Sekoguchi, *Intern. J. Multiphase Flow*, 2, No. 1 (1975).
6. V. M. Kashcheev and Yu. M. Muranov, *Teplofiz. Vys. Temp.*, 14, No. 5 (1976).
7. L.-S. Tong, *Boiling Heat Transfer and Two-Phase Flow*, Wiley, New York (1965).
8. S. S. Kutateladze and A. I. Leont'ev, *Turbulent Boundary Layer of a Compressible Gas* [in Russian], *Izd. Sibirsk. Otd. Akad. Nauk SSSR, Novosibirsk* (1962).
9. S. S. Kutateladze and A. I. Leont'ev, *Heat and Mass Transfer in a Turbulent Boundary Layer* [in Russian], *Énergiya, Moscow* (1972).
10. D. N. Vasil'ev, "Theoretical study of a turbulent boundary layer with a longitudinal pressure and injection," *Author's Abstract of Candidate's Dissertation, Gor'kii* (1975).
11. N. Zuber, F. W. Staub, and G. W. Bijwaard, in: *Advances in Heat Transfer* [Russian translation], *Mir, Moscow* (1970).
12. E. M. Novokhatskii, *Izv. Vyssh. Uchebn. Zaved., Énerg.*, No. 4 (1961).
13. J. R. S. Thom, *Intern. J. Heat Mass Transfer*, 7, No. 7 (1964).

## GAS DISTRIBUTION IN A DEEP GRANULAR BED INJECTED BY FLAT JETS

Yu. A. Buevich, N. A. Kolesnikova,  
and A. N. Tsetovich

UDC 66.096.5

The gas-flow distribution is examined for a set of identical equidistant flat jets entering a deep immobile or fluidized bed.

There is considerable engineering interest in the distribution of the gas injected as jets into a granular bed; this applies particularly in the simulation of exchange in catalytic reactors and other equipments. Also, the gas distribution is extremely important to jet fluidization, which tends to occur with many existing gas-distributing grids, and also has a bearing on the structure of the bed near the wall in the fluidized state, as well as on the shape of any stagnant zones, and so on.

A general method has been given [1] for solving two-dimensional problems in gas distribution. Here we use the basic assumptions of [1]: it is supposed that we can neglect the variation in the dynamic gas pressure along the jets by comparison with the pressure change within the dense phase of the bed, in which case the pressure within a jet may be taken as constant. The hydraulic resistance to the flow entering the dense phase is taken as a linear function of the infiltration speed, while the coefficient of proportionality is independent of the coordinates, i.e., we consider a linear case in infiltration theory. Since the gas speed is usually much greater than the speed of the regular particle motion in the dense phase, we consider the latter as an immobile porous body. The effects of the upper boundary of the bed are neglected, which is justified if the height of each jet is much less than the height of the bed.

The jets are considered as entering from the bottom upward and may be simulated [1] by means of a system of sections  $x' = 2nLh$ ,  $0 \leq y' \leq h$  ( $n = 0, \pm 1, \pm 2, \dots$ ) in the complex plane  $z' = x' + iy'$ ; within the framework of this external treatment [1], the length  $h$  of a section, which characterizes the height of the jets, is taken as given a priori. Some information has been published [2] on the dependence of  $h$  on the dimensions of the injection slots, the bed parameters, and the gas speed at the slot level. Also,  $Lh$  is equal to half the distance between the jets.

---

Institute of Problems of Mechanics, Academy of Sciences of the USSR, Moscow, Moscow Chemical-Engineering Institute. Translated from *Inzhenerno-Fizicheskii Zhurnal*, Vol. 35, No. 3, pp. 424-431, September, 1978. Original article submitted October 26, 1977.